

Stars beyond Galaxies: The Origin of Extended Luminous Halos around Galaxies

Mario G. Abadi,^{1*} Julio F. Navarro,^{1,3†} and Matthias Steinmetz²

¹*Department of Physics and Astronomy, University of Victoria, Victoria, BC V8P 5C2, Canada*

²*Astrophysikalisches Institut Potsdam, An der Sternwarte 16, Potsdam 14482, Germany*

³*Max-Planck Institut für Astrophysik, Karl-Schwarzschild Strasse 1, Garching bei München, D-85741, Germany*

ABSTRACT

We use numerical simulations to investigate the origin and structure of the luminous halos that surround isolated galaxies. These stellar structures extend out to several hundred kpc away from a galaxy, and consist of stars shed by merging subunits during the many accretion events that characterize the hierarchical assembly of galaxies. Such origin suggests that outer luminous halos are ubiquitous and that they should appear as an excess of light over extrapolations of the galaxy’s inner profile beyond its traditional luminous radius. The mass profile of the accreted stellar component is well approximated by a model where the logarithmic slope steepens monotonically with radius; from $\rho \propto r^{-3}$ at the luminous edge of the galaxy to r^{-4} or steeper near the virial radius of the system. Such spatial distribution is consistent with that of Galactic and M31 globular clusters, suggesting that many of the globulars were brought in by accretion events, in a manner akin to the classic Searle-Zinn scenario. Luminous halos are similar in shape to their dark matter counterparts, which are only mildly triaxial and much rounder than dark halos formed in simulations that do not include a dissipative luminous component. The outer stellar spheroid is supported by a velocity dispersion tensor with a substantial and radially increasing radial anisotropy; from $\sigma_r^2/\sigma_t^2 \sim 2$ at the edge of the central galaxy to ~ 5 at the virial radius. These properties distinguish the stellar halo from the dark matter component, which is more isotropic in velocity space, as well as from some tracers of the outer spheroid such as satellite galaxies. Most stars in the outer halo formed in progenitors that have since merged with the central galaxy; very few stars in the halo are contributed by satellites that survive as self-bound entities at the present. These features are in reasonable agreement with recent observations of the outer halo of the Milky Way, of M31, and of other isolated spirals, and suggest that all of these systems underwent an early period of active merging, as envisioned in hierarchical models of galaxy formation.

Key words: Galaxy: disk – Galaxy: formation – Galaxy: kinematics and dynamics – Galaxy: structure

1 INTRODUCTION

Galaxies have no edge. With rare exceptions, the stellar spatial distribution in normal galaxies shows little sign of a sharp outer cutoff, and is reasonably well approximated by density laws that extend smoothly to arbitrarily large radius. Extrapolations of the inner luminosity profile, however, suggest that little light comes from regions of surface brightness much fainter than those traditionally used to define the luminous radii of galaxies (~ 25 mag/arcsec²). Perhaps because of this reason, together with the obvious observational difficulties inherent to studying regions of low-surface

brightness, the outer luminous halos of external galaxies have in the past been regarded as a topic of little more than academic interest.

This impression, however, is rapidly changing, as new datasets start to unveil some unexpected properties of the stellar component that populates the outer confines of galaxies. These developments have been made possible by the development of panoramic digital cameras able to map the light distribution of external galaxies down to unprecedented surface brightness levels, complemented by efficient observational techniques designed to identify and measure radial velocities of outer halo tracers in external galaxies, such as planetary nebulae (PNe, Romanowsky et al. 2003). Finally, the advent of efficient spectrographs in 10m-class telescopes have enabled the measurement of radial velocities of large samples of giant stars throughout the Local Group (Ibata et al 2004), and dedicated

* CITA National Fellow, on leave from Observatorio Astronómico de Córdoba and CONICET, Argentina.

† Fellow of CIAR and of the J. S. Guggenheim Memorial Foundation.

spectroscopic campaigns targeted on giant stars have dramatically increased the sample of tracers in the outer halo of our own Milky Way (Morrison et al 2003, Battaglia et al 2005, Clewley et al 2005).

Likewise, the use of stacking techniques in wide-field surveys such as the Sloan Digital Sky Survey (SDSS) have led to clear detections of a distinct low surface brightness component around both isolated spiral galaxies (Zibetti, White & Brinkmann 2004) as well as central cluster galaxies (Zibetti et al 2005). The surface brightness profile of these outer luminous halos deviate significantly from straightforward extrapolations of the laws that describe the main body of the galaxy, and suggest that estimates of the amount of light in the intergalactic or intracluster medium might need to be revised upward. In the case of clusters, for example, Zibetti et al (2005) conclude that of order 11% of the light in a typical Abell cluster might be in the form of an intracluster luminous component with structural properties distinct from those of the galaxy cluster population and of the central cluster galaxy.

These studies have brought about several unexpected results that challenge some of the accepted premises of the currently accepted galaxy formation paradigm. For example, the kinematics of PNe in the vicinity of several normal ellipticals has been found to be consistent with simple models where such galaxies have no surrounding dark matter halo (Romanowsky et al. 2003, but see Dekel et al 2005). This result, if confirmed by further studies, would be very difficult to accommodate in the Λ CDM scenario, where *all* galaxies are envisioned to form as a result of the dissipative collapse of baryons within massive dark matter halos.

In the case of the Local Group, wide field photometric surveys (and their follow-up spectroscopic campaigns) have modified radically the traditional view of the outer stellar spheroid of the Milky Way and M31. Giant structures interpreted as tidal streams of disrupted or disrupting dwarfs have been identified in both galaxies (Ibata et al 1994, Helmi et al 1999, Majewski et al 2003, Ibata et al 2004), and have solidified the notion that accretion events may play a substantial role in the shaping of individual galaxies. These streams are expected to be short-lived as readily identifiable structures on the sky (Johnston et al 1995, Helmi & White 1999), and, although impressive, they are thought to contribute a relatively small fraction of stars in the halo of these systems. In broad terms, the main characteristics of the outer stellar halo are probably adequately captured by a simple model of a reasonably well-mixed spheroid of stars.

Extensive spectroscopic surveys of giant stars in the outskirts of Local Group galaxies have unraveled some intriguing dynamical properties for the outer halo component. For example, just like PNe around ellipticals, the velocity dispersion of these halo tracers drops significantly in the outer regions of the Milky Way (Battaglia et al 2005, Clewley et al 2005). This is a somewhat unexpected result if these galaxies are embedded in extended dark matter halos, and has prompted renewed interest in the extent and spatial distribution of dark matter in the outskirts of galaxies.

From a theoretical point of view, the interest elicited by outer luminous halos stems from the fact that, in the currently accepted paradigm, stars are envisioned to form only in the collapsed, high-density regions near the center of dark halos—which we identify with the main body of individual galaxies. This prejudice is supported by observations that indicate the need for a threshold gas density below which stars do not form (Kennicutt 1989, Martin & Kennicutt 2001, Schaye 2004), and imply that outer halo stars did *not* form *in situ* but have been shed from protogalaxies during the merger events that characterize the assembly of galaxies in a hierarchically clustering universe.

In simple words, stars found as far away as, say, 100 kpc from a galaxy's center originate in satellites whose orbital apocenter was about that large before they spiraled in to merge with the main galaxy. We therefore expect a clear connection between the orbital properties of stars in the outer halo and those of the progenitors that merged to form the present-day galaxy. Unraveling the structure of the outer luminous halo of galaxies may thus be seen as an important step toward unraveling the merging history of individual galaxies.

In this paper, we analyze the origin and structure of the luminous halos of galaxies simulated in the Λ CDM scenario. We describe briefly in Section 2 the numerical simulations. The main results of our analysis are presented in Section 3 and discussed in § 4. We conclude with a brief summary in Section 5.

2 THE NUMERICAL SIMULATIONS

We analyze a suite of eight numerical simulations of the formation of galaxies in the Λ CDM scenario. These simulations have been analyzed in earlier papers, which may be consulted for details on the code used as well as on the numerical setup (Steinmetz & Navarro 2002, Abadi et al 2003a,b, Meza et al 2003, 2005). In brief, each simulation follows the evolution in a Λ CDM universe of a small region surrounding a target galaxy, excised from a large periodic box and re-simulated at higher resolution preserving the tidal fields from the whole box. The simulation includes the gravitational effects of dark matter, gas and stars, and follows the hydrodynamical evolution of the gaseous component using the Smooth Particle Hydrodynamics (SPH) technique (Steinmetz 1996). We adopt the following cosmological parameters for the Λ CDM scenario: $H_0 = 65$ km/s/Mpc, $\sigma_8 = 0.9$, $\Omega_\Lambda = 0.7$, $\Omega_{\text{CDM}} = 0.255$, $\Omega_{\text{bar}} = 0.045$, with no tilt in the primordial power spectrum. All simulations start at redshift $z_{\text{init}} = 50$, have force resolution of order 1 kpc, and mass resolution so that each galaxy is represented, at $z = 0$, with $\sim 125,000$ star particles.

Dense, cold gas in collapsed regions is allowed to turn into stars at rates consistent with the empirical Schmidt-like law of Kennicutt (1998). The energetic feedback of evolving stars is included mainly as a heating term on the surrounding gas, but the short cooling times in these regions reduce significantly the effectiveness of feedback in curtailing star formation. The transformation of gas into stars thus tracks closely the rate at which gas cools and condenses at the center of dark matter halos. As discussed in the references listed in the above paragraph, this results in an early onset of star-forming activity in the many progenitors of the present-day galaxy present at high redshift. This leads to the formation of a prominent spheroidal component as these progenitors coalesce and merge to form the final galaxy. Gas accreted after the merging activity abates leads to the formation of a centrifugally-supported gaseous and stellar disk component clearly present in most of our simulations, although they make up typically only about $\sim 30\%$ of the final stellar mass of each galaxy.

It is likely that improvements to our feedback algorithms may lead to revisions in the efficiency and timing of star formation in these galaxies. As we discuss below, outer halo stars originate mainly in the merger of the early progenitors, so reducing the efficiency of early star formation should have some impact on the actual prominence of the outer stellar halo component. We expect, however, that reasonable modifications of the star formation algorithm will affect mainly the number, ages, and chemical composition of outer halo stars, rather than its dynamical and structural

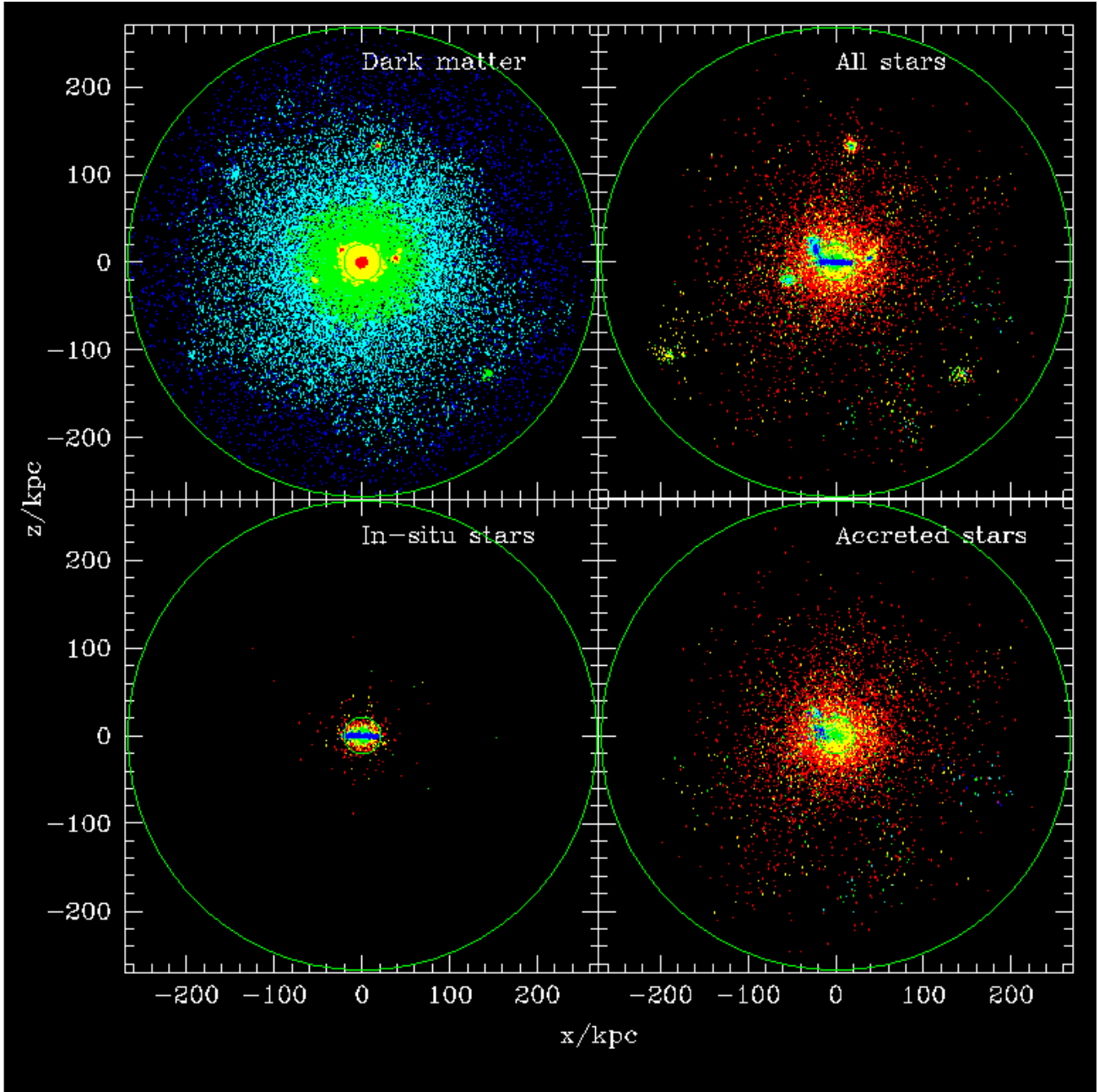


Figure 1. Spatial distribution of the dark matter and stellar component of one simulated galaxy at $z=0$. Top panels show the dark matter (left) and the stars (right) within the virial radius of the system. Dark matter particles are colored by their local density, whereas stars are colored by age (blue: $0.0 < \text{age/Gyr} < 2.5$, cyan: $2.5 < \text{age/Gyr} < 5.0$, green: $5.0 < \text{age/Gyr} < 7.5$, yellow: $7.5 < \text{age/Gyr} < 10.0$, red $10.0 < \text{age/Gyr} < 15.0$). The outer green circle shows the virial radius of the system, the inner circle shows the radius adopted as the “luminous radius” of the galaxy. Bottom panels split the stellar component into two different groups: stars formed in the main progenitor of the galaxy (i.e., “in situ” stars, left panel) and those contributed by accretion events (“accreted” stars, right panel). The latter group excludes stars in satellites that remain self-bound in the halo of the galaxy.

properties, which we expect to depend mainly on the orbital properties of the merging progenitors and on the structure of the dark matter halo host. These properties are less sensitive to the complex astrophysics of star formation and feedback, and we therefore focus our analysis on the structure and dynamics of the outer stellar halo in our eight simulations. These target a small range in mass chosen so that at $z = 0$ the galaxies have luminosities and circu-

lar speeds comparable to the Milky Way. We summarize the main structural parameters of the dark matter and stellar components of the simulated galaxies in Table 1.

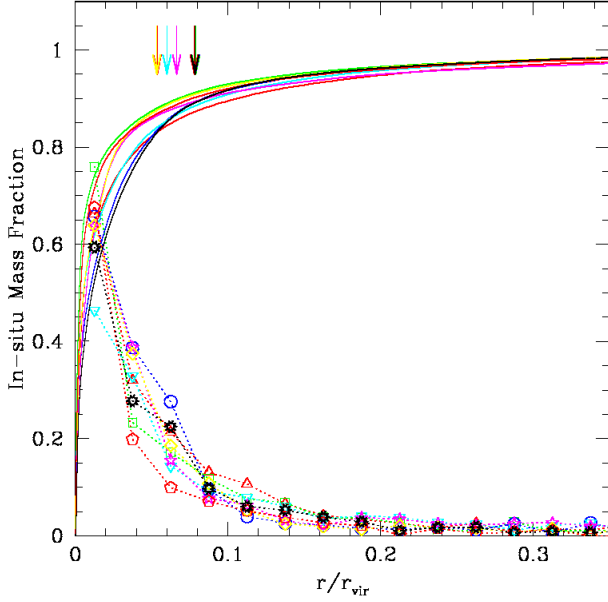


Figure 2. The radial dependence of the fraction of stars formed in the most massive progenitor of the final galaxy (i.e., stars formed *in situ*) is indicated by dotted lines connecting symbols. The thick solid lines indicate the cumulative fraction of stars within the virial radius. In-situ stars dominate throughout the main body of the galaxy; within the “luminous radius” of the galaxy, defined to be $r_{\text{lum}} = 20$ kpc (shown with arrows), they contribute $\sim 60\%$ of the stellar mass. Outside r_{lum} the stellar component consists almost exclusively of accreted stars; indeed, fewer than $\sim 5\%$ of stars in the outer ($r > r_{\text{lum}}$) halo formed in situ.

3 RESULTS

Figure 1 shows, at $z = 0$, one of our simulated galaxies (KIA3, see Table 1) projected onto a box of 540 kpc on a side. The top panels show the dark matter particles (left) and stars (right) within the virial radius ($r_{\text{vir}} \approx 270$ kpc, shown by the outer green circle), defined to encompass a region of mean density 100 times the critical density for closure. Dark matter particles are coloured by their local density, while stars are coloured by their age, as described in the label.

The bottom panels in Figure 1 separate the stars in two components: “in situ” stars that formed in the most massive progenitor (left) and “accreted stars” that formed in progenitors that merged with the main galaxy (right). Stars labelled as “accreted” exclude those associated with self-bound satellite systems that survive until the present. These can be seen clearly in the top-right panel of Figure 1, but are largely absent in the bottom-right panel, except for a sprinkling of stars associated with a young stream recently torn from a disrupting satellite, visible at $x \sim -20, y \sim 10$ kpc. Roughly $\sim 48\%$ of stars (by mass) formed “in situ” in this galaxy, compared with $\sim 44\%$ which make up the accreted component. Satellites contribute a rather small fraction ($\sim 8\%$) of all stars within r_{vir} . These numbers are typical of our simulations, as may be seen from the numbers listed in Table 1.

Figure 1 illustrates a number of properties of the stellar component common to all of our simulations. In particular, it is important to note that (i) stars spread as far out as the virial radius of the system (outer circle in the panels of Figure 1), although they are more highly concentrated than the dark matter halo; (ii) *in situ*

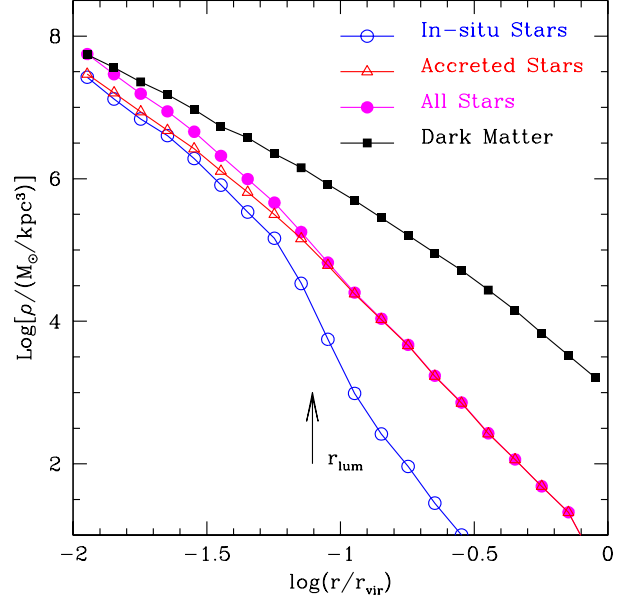


Figure 3. Density profile of stars (circles) and dark matter (squares) in one of our simulations (KIA3), shown in a logarithmic scale. Open circles correspond to the stars formed in situ, whereas filled circles correspond to accreted stars. Note that the *shape* of the density profile of the accreted stellar component is similar to that of the dark matter, and can be adequately fit with a radial law where the logarithmic slope is a power law of radius. See text for details.

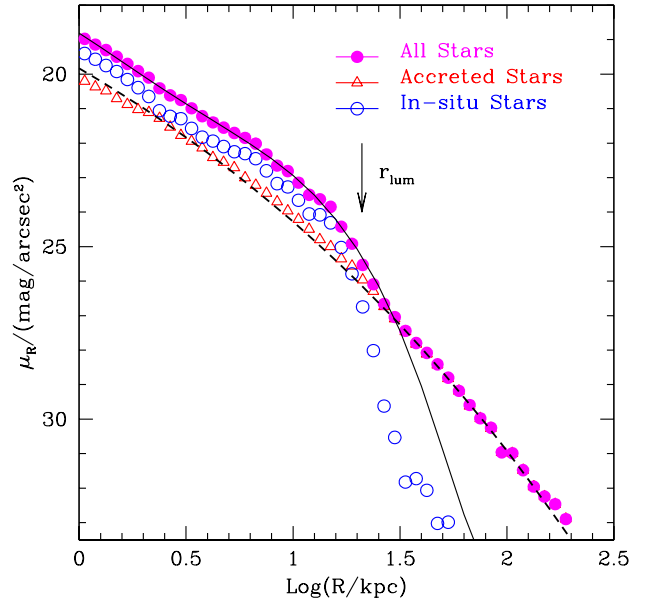


Figure 4. R -band surface brightness profile of stars, split between the “in-situ” and “accreted” components (run KIA3, see Table 1). The accreted stars dominate outside the luminous radius and appear as an excess of light over a bulge+disk fit to the inner surface brightness profile, which is shown as a solid line. The dashed line shows a Sersic-law fit to the outer profile of accreted stars. Note that a single Sersic-law (with parameters given in Table 2) reproduces very well the radial distribution of all accreted stars.

stars (bottom left panel), are responsible for most of the young stars in the main body of the galaxy (note the prominence of the young disk in the bottom-left panel), and are practically absent from the outer halo; whereas (iii) accreted stars (bottom right panel) make up preferentially the spheroidal component and dominate the stellar budget in the outer regions of the galaxy.

The relative importance of the “accreted” vs “in situ” components at various radii is shown in Figure 2. Beyond a radius $r_{\text{lum}} = 20$ kpc (marked by arrows in Figure 2) accreted stars dominate in all our simulations. We shall define r_{lum} as the “luminous radius” of the galaxy and refer to stars beyond r_{lum} as the “outer luminous halo” or “outer galaxy”, for short. Our analysis focuses on the structure and dynamics of the outer halo and, consequently, mainly on the properties of the accreted component.

It is also clear from this figure that the outer luminous halo contains a relatively small fraction of the stellar mass of the galaxy; fewer than 15% of all stars are found between r_{lum} and the virial radius. We note as well that accreted stars make up a non-negligible fraction of stars in the inner galaxy (i.e., inside r_{lum}); we shall therefore distinguish between “accreted” and “outer halo” stars in what follows.

Figure 3 shows the density profile of the stellar and dark matter components of the simulation shown in Figure 1. The stellar contribution is split between in-situ and accreted stars. Note that stars are significantly more concentrated than the dark matter; indeed, they contribute a significant fraction of the *total* mass within the luminous radius (44% on average for all runs in our series), but they make up a negligible amount of the total mass in the outer regions. Note as well the sharp truncation of in-situ stars at $r > r_{\text{lum}}$; essentially no stars in the outer halo were formed in the main progenitor. This is a natural consequence of the fact that in-situ star formation proceeds efficiently only in regions of high-density. The few in-situ stars found beyond r_{lum} at $z = 0$ have been torn from the main progenitor during mergers, although Figure 2 (and the data in Table 1) shows that this is rather inefficient, and that the “accreted” component dominates the stellar component of the outer halo.

The radius beyond which accreted stars begin to dominate is signaled by an abrupt change in the surface brightness profile of the galaxy, as shown in Figure 4. Inside the luminous radius, where μ_R is brighter than about 25.5 mag/asec², the surface brightness profile of this galaxy (projected in this case face-on and studied in detail by Abadi et al 2003a,b) is well approximated by a de Vaucouleurs bulge plus an exponential disk (shown as a solid line). This bulge+disk model is, however, unable to fit the structure of the outer luminous halo, which deviates from the inner profile and appears as a outer luminous “excess” beyond ~ 30 kpc, where the R -band surface brightness drops to values fainter than about 26.5 mag/asec².

The outer halo surface brightness profile steepens gradually outwards and is well approximated by a Sersic-law,

$$\Sigma(R) = \Sigma_{\text{eff}} e^{-b_n [(R/R_{\text{eff}})^{1/n} - 1]} \quad (1)$$

where R_{eff} and Σ_{eff} are, respectively, the radius containing half the light and the surface brightness level at that radius. The surface brightness profile of the outer regions of our simulated galaxies is shown in Figure 5a, together with Sersic-law fits to the outer portion of the profiles.

The Sersic fit parameters are listed in Table 2. On average we find $\langle n \rangle = 6.3$; $\langle R_{\text{eff}} \rangle = 7.7$ kpc. The outer luminous halo’s surface brightness profile steepens from $\Sigma(R) \propto R^{-2.3}$ at about the luminous radius to $R^{-2.9}$ at $r \sim 100$ kpc and to $R^{-3.5}$ or steeper around the virial radius. The gradually steepening profile of the

outer halo characterized by the Sersic law is reminiscent of the distribution of dark matter, whose density profile also steepens monotonically outward (Navarro et al 2004). The dark matter profile is, however, much less centrally concentrated and its slope is shallower than the stellar halo at all radii. As discussed by Merritt et al (2005), the dark matter density profile may also be approximated by a Sersic law, but with a characteristic value of $2 < n < 4$ and much larger effective radii.

Figure 5b shows the surface brightness profiles of the *accreted stellar component only* for all eight simulations in our series. The profiles have been scaled so that they would all line up along a line of slope -1 if they followed accurately a Sersic law. All profiles are indeed well approximated by eq. 1, with the possible exception of one case where a “bump” of stars associated with an ongoing satellite disruption event is seen just outside R_{eff} (open starred symbols in Figure 5b). This raises the interesting prospect of estimating the *total* fraction of stars accreted throughout the history of a galaxy simply by fitting its outer profile. As the last two columns of Table 2 demonstrate, the total light contributed by accreted stars is well approximated (to within a factor of ~ 2) by the total light of a Sersic-law fit to the outer luminous halo.

The similarity between profiles suggest that the violent relaxation associated with mergers endows the accreted stellar component with a simple, roughly self-similar structure that is well approximated by a Sersic law. This process has been studied extensively in the literature, and previous studies have consistently found that the structure of N-body merger remnants is quite reminiscent to that of bright ellipticals (see, e.g., Barnes & Hernquist 1992 and references therein), which are indeed well approximated by a Sersic law with $n \gtrsim 4$ (see, e.g., Graham & Guzman 2003 and references therein).

One may think of the accreted stellar component as formed by the overlap of the many “tidal tails” stripped from the merging progenitors; in this interpretation the outer luminous halo would just be the superposition of the outer tails stripped from each progenitor during the merger process. This characterization of the accreted stellar component helps to explain the remarkable kinematics of the outer halo shown in Figure 6. This figure shows the velocity dispersion profile of stars and dark matter, averaged over all simulations after scaling the positions and velocities of all particles to the virial radius and virial velocity of each system. The right panels in Figure 6 show that the velocity dispersion of the dark matter declines gradually from the center outwards, and is characterized by a mild radial anisotropy, going from almost isotropic near the center to $\beta = (1 - \sigma_t^2/\sigma_r^2) \sim 0.3$ in the outer regions. (We use σ_t to denote the tangential velocity dispersion; $\sigma_t^2 = (\sigma_\theta^2 + \sigma_\phi^2)/2$.)

The outer luminous halo, on the other hand, shows a much more pronounced radial bias: from $\beta \sim 0.4$ just outside the luminous radius of the galaxy (r_{lum} is on average of order $0.06 r_{\text{vir}}$) to about $\beta \sim 0.8$ near the virial radius. This substantial—and monotonically increasing—radial anisotropy may also be understood as a direct consequence of the tidal disruption process of formation described above. Outer halo stars are typically stripped from merging progenitors during pericentric passages. However, because stars form in high-density regions the stripping of stars operates efficiently only when pericenters are small (and tidal effects are greatest). This occurs typically after dynamical friction has eroded the orbit sufficiently to bring the pericenter of the accreting satellite close to the central galaxy. As a result, outer halo stars are “launched” into highly energetic orbits with, characteristically, the (small) pericentric radii that accompany the most disruptive tides. Stars able to reach farther are thus typically on more eccentric or-

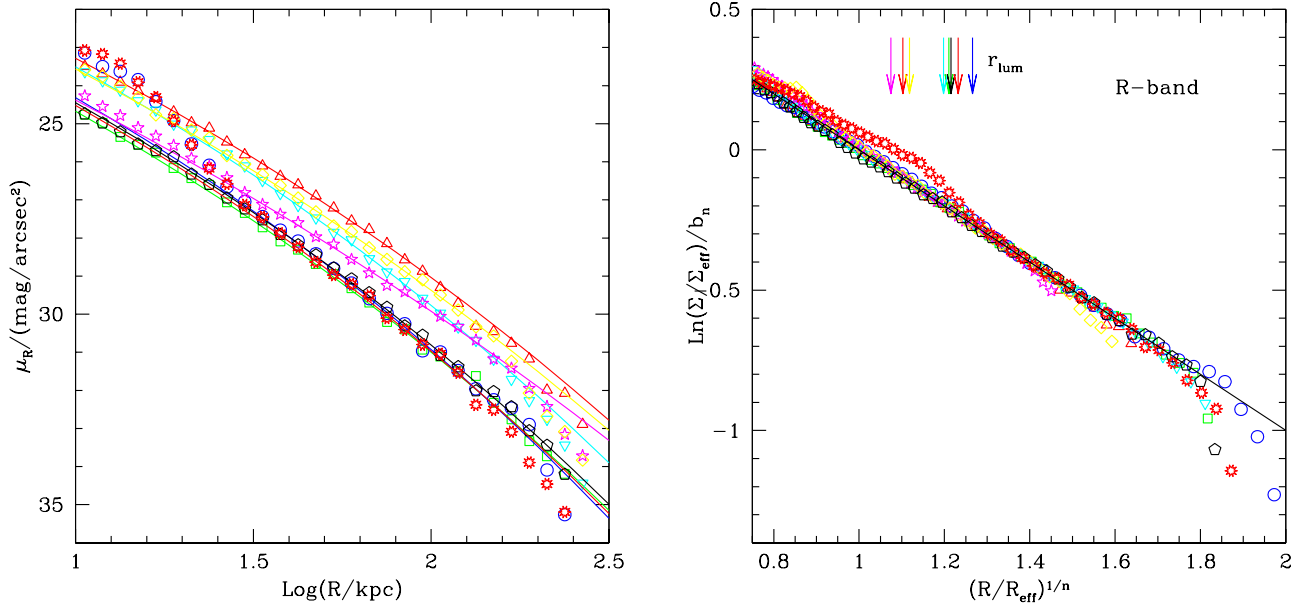


Figure 5. (a-left) R-band surface brightness profile of the outer galaxy ($10 < R/\text{kpc} < 300$) in all of our simulations. Solid lines correspond to the best Sersic-law fits to the outer regions of the profile ($r > r_{\text{lum}}$) whose parameters are listed in Table 2. (b-right) Same as in the left, but profiles correspond *only* to accreted stars and have been scaled as stated in the axis labels so that Sersic-law profiles would follow the straight solid line of slope -1 . Interestingly, a simple Sersic-law reproduces quite well the radial distribution of accreted stars in all simulations. There is one exception (which shows as a bump in the right-hand panel), associated with the transient effect of an ongoing satellite disruption event.

bits, leading to the increasing radial anisotropy in the orbits of the outer halo stars seen in Figure 6.

The formation process of the accreted stellar component is thus qualitatively similar to that of the dark matter halo, where mergers also play a substantial role. It is thus perhaps not surprising that they settle onto similar, mildly triaxial structures, as shown in Figure 7. For the accreted stars, the average intermediate-to-major axis ratio is $\langle b/a \rangle = 0.91$, whereas the average minor-to-intermediate axis ratio is $\langle c/b \rangle = 0.92$ ($\langle c/a \rangle = 0.84$). This is not too different from the dark matter halos, which have on average $\langle b/a \rangle = 0.94$ and $\langle c/b \rangle = 0.90$ ($\langle c/a \rangle = 0.84$). We note that the dark matter halos in these simulations are much rounder than typically found in N-body simulations of CDM halo formation: $\langle b/a \rangle \sim 0.75$ and $\langle c/a \rangle \sim 0.6$ (see, for example, Bailin & Steinmetz 2004). This is the result of the response of the halo to the dissipative assembly of the baryonic component of the galaxy at its center, which steepens the potential well and reduces the triaxiality of the halo; see, e.g., Kazantzidis et al (2004), Bailin et al (2005), and references therein.

The in-situ stellar component, on the other hand, often sports a well defined rotationally-supported disk (see, e.g., lower left panel of Figure 1) and its shape is thus well described by an oblate structure with $\langle b/a \rangle = 0.95$ and $\langle c/a \rangle = 0.62$. Although rotation plays little role supporting the accreted component (the mean rotation velocity, $\bar{v}_\phi = j_z/R$, is typically less than one tenth of the circular velocity at each radius), it is interesting to note that the direction of its angular momentum is well aligned with that of the inner galaxy.

This is shown in Figure 8, which show the distribution of the cosine of the angles between the angular momentum of the dark matter halo (\vec{J}_{dm}), the in-situ stars (\vec{J}_{ins}), and the accreted stellar halo (\vec{J}_{acc}). Although the good agreement between \vec{J}_{acc} and \vec{J}_{ins} could have perhaps been anticipated (after all, they are both part

of the same stellar system) it is still interesting to note the strong correlation between the rotational properties of the inner galaxy and the dark matter halo. This implies that, although mergers lead to substantial transfer of angular momentum from the stars to the dark halo (Navarro & Steinmetz 1997, Abadi et al 2003a), this does not alter radically its orientation, so that the spin of the inner galaxy generally ends up aligned with the rotation axis of the surrounding dark matter halo.

It is also of interest to characterize the orientation of the rotation axis relative to the principal axes of the system. Figure 9 shows the alignment between the galaxy’s angular momentum and the minor axis of the dark matter and luminous halos. No obvious alignment is seen in these panels, suggesting that the rotational properties of the galaxy are, at best, weakly correlated with the shape of the surrounding dark matter (or luminous) halo. We shall return to possible interpretations of this result in the following section.

We end the characterization of the outer luminous halos of simulated galaxies by comparing the age distribution of stars in the inner and outer galaxy, as well as that of satellites enclosed within the virial radius (Figure 10). The ages of stars in the outer galaxy ($r > r_{\text{lum}}$) differ significantly from those in higher density regions (like the inner galaxy or the surviving satellites), where star formation may proceed. The outer halo is populated mainly by older stars, reflecting the fact that the mergers responsible for its formation are more common at earlier times. Interestingly, the distribution of ages of stars in the outer halo is also fairly distinct from that of stars in satellites orbiting within the virial radius. This shows that relatively few stars in the outer halo originate in the “harassment” of satellites that have survived as self-bound entities until the present (Moore et al 1996). Most stars in the outer halo come from merger events whose progenitors have long been fully disrupted, suggesting that the properties of the satellite population may be quite distinct from

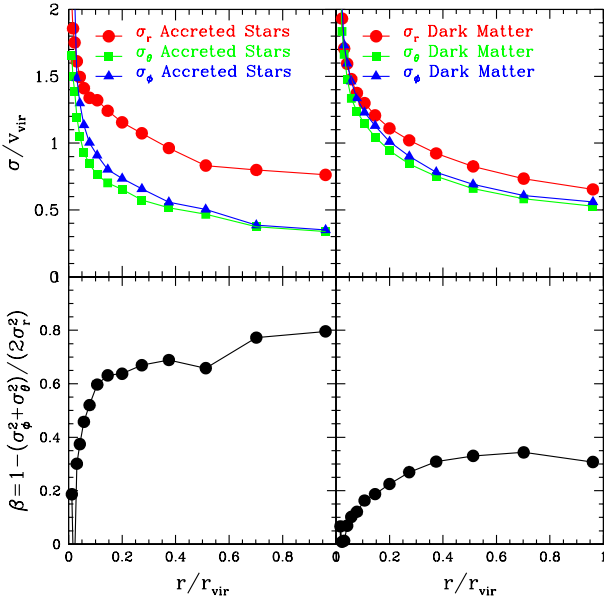


Figure 6. Average velocity dispersion profile of stars and dark matter in our simulations. Averages are computed by scaling all positions and velocities to the virial radius and virial circular velocity of each system, respectively. The rotation axis of the inner galaxy is chosen as the polar axis of the scaling procedure. Particles are then grouped in spherical bins and the spherical components of the velocity dispersion are computed. These profiles are finally averaged over all systems to produce the radial and tangential velocity dispersion profiles plotted here. Right panels correspond to the dark matter component and left panels to the accreted stars. Recall that, on average, the luminous radius is $\sim 0.06 r_{\text{vir}}$ in these units. Note that the dark matter velocity dispersion exhibits a mild radial bias; the radial bias is much more pronounced, and monotonically increasing, in the case of the accreted stellar component.

that of the smooth outer halo. We explore the consequences of these results for the interpretation of observational data in the following section.

4 DISCUSSION

The results presented in the previous section have a number of implications regarding the interpretation of observations of stars in regions far removed from the normal boundaries of typical galaxies. Our simulations suggest that these “intergalactic stars” (or, more properly, “extra-galactic stars”) are a relict of the merging history of each individual galaxy. As such, all galaxies with a past of active merging activity (the majority in a hierarchically clustering scenario such as Λ CDM) should have an outer stellar halo component with properties similar to those described in the previous section.

The outer luminous halo should appear as an excess of light over the extrapolated profile of the inner galaxy. Its structure is characterized by a gradually steepening density profile and by a clearly defined radial anisotropy in the velocity distribution. Outer halos are rather difficult to detect, since they are—by definition—confined to regions of very low surface brightness difficult to probe observationally. However, the presence of outer luminous components detached from the properties of the inner galaxy have been recently reported by a number of authors. Following the pioneering work of Sackett et al (1994), Morrison et al (1994), and Zheng et

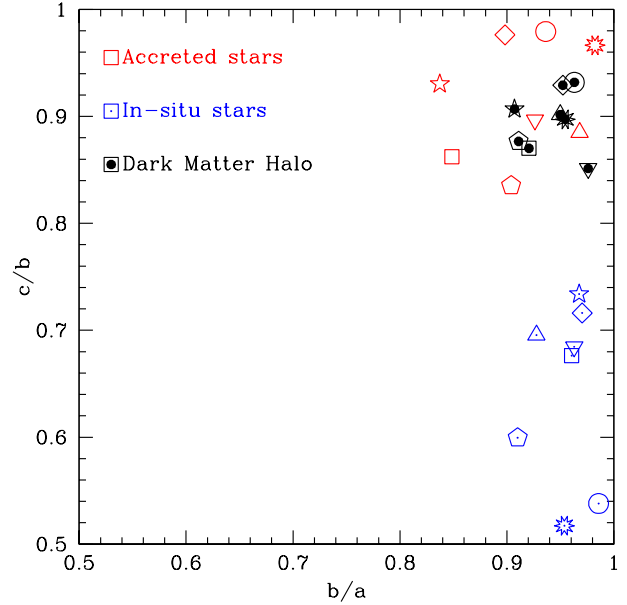


Figure 7. Inertia axis ratios of the dark matter halo, as well as of the accreted and in-situ stellar components. Axis ratios are computed by diagonalizing the inertia tensor $I_{ij} = \sum m_i x_i x_j$ for all particles of each component within the virial radius of the system. Note that the shape of the dark matter and accreted components are similar and only mildly triaxial, but that the in-situ stars are predominantly oblate. This reflects the fact that in-situ stars have a higher proportion of newly formed stars, which tend to arrange themselves in a disk-like structure (see Figure 1).

al (1999) among others, Zibetti, White & Brinkmann (2004), have recently reported the statistical detection of a $\rho \propto r^{-3}$ halo of stars in the outskirts of a sample of edge-on disk-dominated galaxies selected from the Sloan Digital Sky Survey (SDSS).

Encouragingly, this outer halo component is detected as excess light over an extrapolation of the inner disk (see Figure 4); the halo dominates the minor axis light profile beyond about ~ 6 exponential scalelengths, in regions where the r -band surface brightness drops to values fainter than $\mu_r \sim 27.5$. A qualitatively similar result has been derived for M31 through detailed stellar counts by Guhathakurta et al (2005) and by Irwin et al (2005), who find that the surface brightness profile along the minor axis “flattens” relative to an extrapolation of the de Vaucouleurs fit to the inner spheroid at radii beyond ~ 20 kpc.

Our simulations provide a compelling interpretation where outer stellar halos are made up predominantly of stars accreted during previous merger events and, in particular, by the subset which were propelled into highly energetic (and highly eccentric) orbits during the disruption process that accompanies the mergers. Mergers and phase mixing lead then to the formation of a tenuous, distinct stellar component that fills the halo of the galaxy out to the virial radius.

Although we expect them to be ubiquitous, the prominence of these outer luminous halos is difficult to assess from a theoretical point of view, as it depends critically on the number and timing of merger events, as well as on the fraction of stars present at the time the mergers occur, all of which remain highly uncertain. A number of general inferences are, however, still possible. Late major mergers should propel a proportionally larger fraction of stars into the outer halo, and therefore the relative prominence of this component

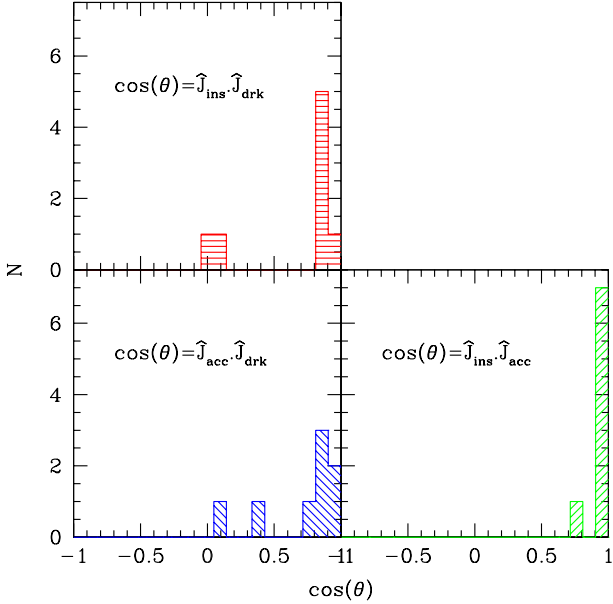


Figure 8. Distribution of the cosine of the angle between the angular momentum vector of the in-situ stellar component, \vec{J}_{ins} , the accreted stars, \vec{J}_{acc} , and the dark matter, \vec{J}_{drk} . Each of the three different permutations are shown by different shaded histograms, as indicated in the labels of each panel.

should be higher in spheroid-dominated galaxies, which are widely regarded as merger remnants. This process should be especially important in systems that have undergone repeated mergers, leading to the expectation that the relative importance of the “intracluster” stellar component should be highest in clusters with prominent cD galaxies.

In disk-dominated galaxies, where in-situ star formation is typically still ongoing and mergers are less important, the outer halo is likely to dominate the profile only at large radii, where star formation thresholds prevent the efficient formation of in-situ stars (Kennicutt 1989, Ferguson et al 1998, Schaye 2004). The accreted stellar component—to which no such threshold applies—appears then as a distinct outer component, “flattening” the surface brightness profile in the outer regions, as reported by Zibetti et al (2004), Guhathakurta et al (2005) and Irwin et al (2005).

Quantitatively, we expect the slope of the surface brightness profile of the outer luminous halo to steepen gradually outwards, as dictated by the Sersic-law fits summarized in Table 2. Given that the average effective radii of the accreted component is 7.7 kpc and $\langle n \rangle = 6.3$, we expect its surface brightness profile to steepen from from $\Sigma \propto R^{-2.2}$ at the luminous radius (20 kpc) to $\Sigma \propto R^{-2.9}$ at $r \sim 100$ kpc. This is in reasonable agreement with the results of Zibetti et al (2004), Irwin et al (2005), and Guhathakurta et al (2005). The latter authors, in particular, report that the M31 outer halo may be approximated by $\Sigma \propto R^{-2.3}$ in the range 30 kpc $< R < 100$ kpc, slightly shallower than in our simulations, but not inconsistent given the substantial observational uncertainty.

We note as well that the distribution of globular clusters in the Milky Way and M31 is consistent with that of the accreted stellar component in the simulations. With the caveat of small number statistics (only ~ 150 globular clusters around the Galaxy and ~ 360 around M31 are currently confirmed; see Harris 1996 and

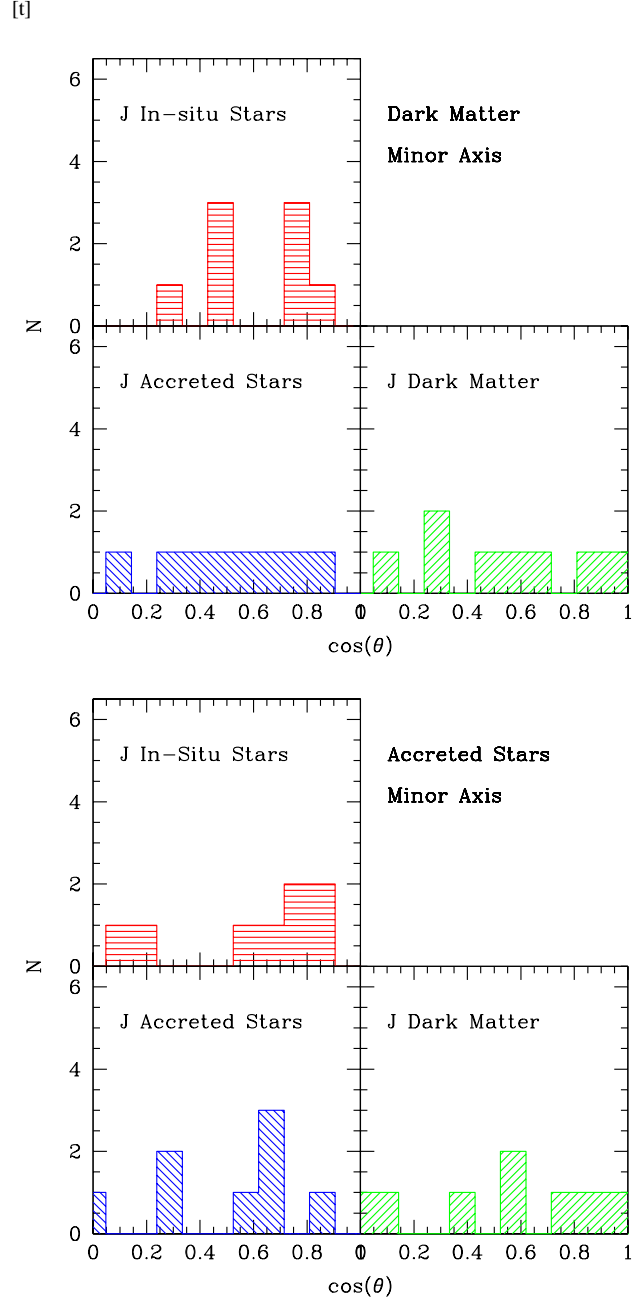


Figure 9. (a)-top: Distribution of the cosine of the angle between the angular momentum of in-situ stars, \vec{J}_{ins} , accreted stars, \vec{J}_{acc} , and the dark matter, \vec{J}_{drk} , and the minor axis of the dark matter. As in Figure 8, histograms of different shades refer to the various permutations, as indicated in the labels. (b)-bottom: Same as (a), but for the minor axis of the accreted stellar component.

Galleti et al 2004), it is interesting that a Sersic law with $n \sim 6$ is consistent with the (projected) number density profile of Galactic globulars. This is shown in Figure 11, where the profile of M31 and Galactic globulars is compared with the Sersic-law that describes the average accreted stellar component in our simulations. We emphasize that the curves shown are *not* fits, and therefore the general agreement is quite suggestive. A simple interpretation, of course, is that the globular cluster population shares the same “external”

origin as that of accreted stars in our simulations, and that they are thus relicts of the accretion history of each galaxy. (Guhathakurta et al (2005) note as well that the smooth halo of M31 red giant stars they detect out to ~ 150 kpc mimics the distribution of its globular cluster population.) Taken together, the evidence linking globular clusters with accretion events, as envisioned in the classic model of Searle & Zinn (1978), seems quite strong.

In terms of space density, the slope of the accreted stellar component is close to $\rho \propto r^{-3.1}$ near the edge of the luminous galaxy. This is in reasonably good agreement with that inferred from tracers of the stellar halo of the Milky Way in the vicinity of the Sun (see, e.g., Zinn 1985, Saha 1985, Morrison et al 2000). Our simulations imply that the halo profile should steepen gradually with radius and become significantly steeper than r^{-3} in the outer regions. It is interesting to explore the consequences of this gradual steepening for the interpretation of dynamical data in the outskirts of the Milky Way.

Battaglia et al (2005) report that the velocity dispersion of halo tracers such as blue horizontal branch stars and red giants declines from ~ 120 km/s at the edge of the luminous disk to ~ 50 km/s at ~ 120 kpc. These authors argue that the data favour a dark matter halo model sharply truncated in the outer regions over the extended mass distributions predicted for CDM halos, such as the Navarro, Frenk & White (1996, 1997, NFW) profile. Neither halo model, however, is completely satisfactory. Extreme radial velocity anisotropy ($\beta \sim 1$) is required to reconcile the data with an NFW halo model although the opposite (i.e., a tangentially anisotropic velocity distribution, $\beta \sim -0.5$) is required for the truncated halo model. The latter seems an unlikely result given that the outer regions of systems assembled hierarchically are typically dominated by radial motions (see, e.g., Hansen & Moore 2004 and references therein).

We can use our results to explore the consistency of the velocity dispersion data with CDM halos. We write the spherical Jeans' equation as,

$$V_c^2(r) = -\sigma_*^2 \left(\frac{d \ln \rho_*}{d \ln r} + 2\beta_*(r) + \frac{d \ln \sigma_*^2}{d \ln r} \right), \quad (2)$$

where we have used a * subscript to denote quantities associated with the stellar halo. The terms in the left-hand side of eq 2 may be evaluated by combining the Battaglia et al data with the assumption that the stellar halo profile may be approximated by a Sersic-law with the (average) parameters given in Table 2. The result of this exercise is shown in Figure 12.

Interestingly, this simple model predicts a circular velocity near the center consistent with that measured at the solar circle (~ 220 km s $^{-1}$) without tuning (solid squares in the bottom panel of Figure 12). Further out, the sustained drop in σ_* leads to much lower circular velocities, approaching ~ 150 km s $^{-1}$ at $r \sim 100$ kpc. This drop in the circular velocity of the system illustrates why Battaglia et al's analysis favours a truncated halo. We argue, however, that the data are consistent with an extended CDM halo, and that the velocity dispersion drop places interesting constraints on its total mass.

This is shown in the bottom panel of Figure 12 by the top thick solid line, which corresponds to an (adiabatically contracted) NFW halo of virial velocity $V_{\text{vir}} = 110$ km/s and concentration $c = 14$ (the average for halos of this mass in the Λ CDM cosmogony). The halo contribution before and after contraction is shown by the dotted and dashed lines, respectively.

The relatively good agreement with the V_c profile derived from the data implies that, rather than being truncated, the halo

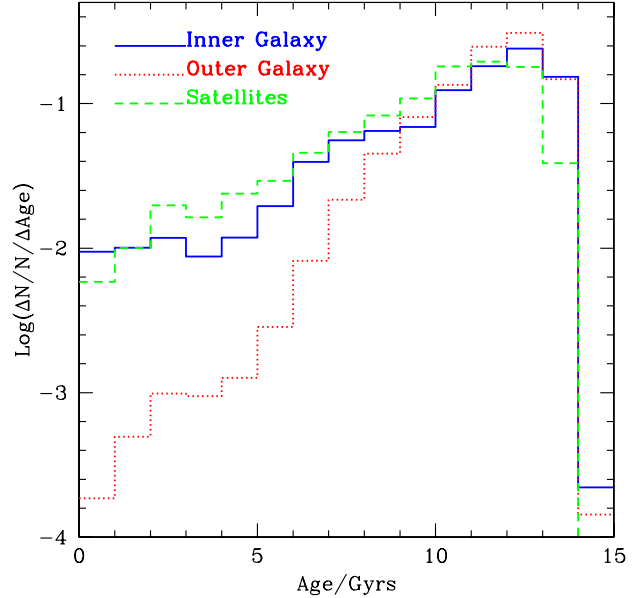


Figure 10. Age distribution of stars in the inner galaxy (i.e., stars within r_{lum} , solid blue line), in the outer galaxy ($r > r_{\text{lum}}$, dotted red line) and in satellites (dashed green line) enclosed inside the virial radius r_{vir} and averaged over our set of 8 simulations.

of the Milky Way may just be less massive than commonly assumed. The virial mass of the fit shown in Figure 12 is only $\sim 6.4 \times 10^{11} M_{\odot}$, and its virial velocity is only one half of the circular speed at the solar circle. This result is similar to that of Klypin, Zhao & Somerville (2002), who analyzed constraints placed by dynamical tracers within the luminous radius of the Milky Way and found that reconciling such data with CDM halos requires the virial velocity of the dark matter halo to be substantially lower than the rotation speed of the disk. (Their favourite Milky Way halo model has $M_{\text{vir}} \approx 10^{12} M_{\odot}$, which corresponds to $r_{\text{vir}} \approx 260$ kpc, and $V_{\text{vir}} \approx 130$ km s $^{-1}$.) One may rephrase this result by stating that the relatively small dark matter contained within the luminous radius of the Galaxy is easiest to accommodate with low-mass halo models, which have the virtue of predicting directly a sharp drop in the velocity dispersion of outer halo tracers. A similar argument was developed by Navarro & Steinmetz (2000), although note the erratum presented in Eke, Navarro & Steinmetz (2001).

It is unclear whether the mass of the halo of the Milky Way is unusually low compared with other spiral galaxies of similar luminosity, but galaxy-galaxy weak lensing data seem to favour halo masses of the order we find here for late-type L_* galaxies (see, e.g., Guzik & Seljak 2002). Also, there is now convincing evidence that the velocity dispersion of satellite galaxies drops at large projected radii so the drop in V_c in the outer regions may actually be a common feature in Milky Way-like galaxies (see Brainerd 2004 for a review).

Turning our attention now to the velocity structure of the outer halo, we recall the pronounced radial anisotropy shown in Figure 6, and argue that such effect should not be ignored when interpreting the dynamics of halo tracers in the outskirts of galaxies. As shown by Dekel et al (2005), accounting for such anisotropies may be enough to reconcile the steeply declining velocity dispersion profiles of planetary nebulae around bright ellipticals (Romanowsky

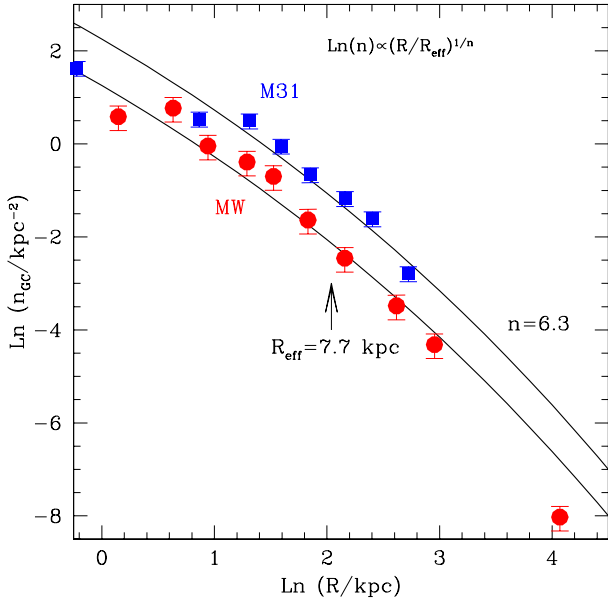


Figure 11. Projected number density profile of globular clusters around the Milky Way (filled circles) and M31 (filled squares), respectively. Data for the 147 Galactic globulars and for the 363 M31 globulars are from Harris (1996) and Galleti et al (2004). We assume that 100 arcmin = 22 kpc at the distance of M31. We have averaged the distribution of Galactic globulars over several random lines of sight to construct the projected number density profile. Each bin contains 15 and 40 globulars for the Galaxy and M31, respectively, and has Poisson error bars. The two curves are *not* fits to the data; rather, they illustrate the distribution of accreted stars in our simulations. Parameters for the two Sersic-law curves are chosen to be the average of the data presented in Table 2 and are vertically scaled to match the data for each galaxy.

et al. 2003) with the presence of massive dark halos around these objects. The radial anisotropy differentiates dynamically the stars in the outer halo from the dark matter (Figure 6). It also distinguishes the stellar halo from the population of surviving satellites, which are found to trace rather faithfully the main properties of the dark halo. Indeed, the average anisotropy of the satellite population in our simulations is found to be $\beta \sim 0.45$ (Sales et al, in preparation), closer to that of the dark matter, and certainly less anisotropic than the accreted stellar component.

This dynamical distinction is not surprising, as we find that the smooth stellar halo has little relation with the population of surviving satellites (see Figure 10). Indeed, few stars in the outer halo may be traced to satellites that survive as self-bound entities until the present. The properties of the stellar halo seems more closely linked to the progenitors of early mergers than to the “harassment” of the satellite population that survives until the present day.

This result has interesting consequences when applied to the interpretation of the origin of the intracluster light (ICL) component. Zibetti et al (2005), for example, find that the properties of the ICL in their sample of clusters selected from the SDSS are quite different from those of the cluster galaxy population as a whole. In particular, the ICL is found to be more centrally concentrated than the cluster galaxies and more significantly aligned with the (brightest cluster galaxy (BCG) than cluster galaxies. In other words, the ICL seems more intimately related to the central galaxy (BCG) than to the cluster galaxy population. All of these properties are consis-

tent with a scenario where the origin of the ICL is traced to the mergers that led to the formation of the BCG, with a minor contribution from stars stripped from surviving galaxies.

A final item for discussion is the weak alignment between dark halo shapes and angular momentum shown in Figure 9. At first, this seems in disagreement with previous studies, many of which report significant alignment between the rotation axis and the minor axis of CDM halos (see, e.g., Bailin & Steinmetz 2004 and references therein). The issue may be resolved by noting that the shapes of the dark halos change dramatically when a dissipative baryonic component is included; indeed, in most cases the dark halos are so nearly spherical that the precise directions of the principal axes are poorly determined. Furthermore, as discussed by Bailin et al (2005), it appears as if the *inner* regions of the dark matter halo respond to the assembly of the galaxy by aligning its minor axis with that of the luminous component, but at the same time decouple from the orientation of the halo in the outer regions.

Interestingly, the weak correlations between halo shape and spin that our simulations predict could be tested directly with upcoming weak lensing surveys. Hoekstra et al (2004) report a tantalizing correlation between the shape of the luminous galaxy and that of their surrounding matter, but their sample contains a broad mixture of morphological types and a relatively strong contribution from spheroid-dominated galaxies, where the relationship between shape and spin is less clear than in spiral galaxies. Weak lensing analysis applied to spiral-dominated samples should provide further constraints on this topic. This is currently being addressed using large, morphologically-segregated samples from the SDSS (Mandelbaum et al, in preparation).

5 SUMMARY

We investigate the origin of stars that populate regions well beyond the traditional luminous boundaries of normal galaxies using numerical simulations of galaxy formation in the Λ CDM cosmogony. Our simulations shows that such components are ubiquitous and owe their presence to the many mergers that characterize the early formation history of galaxies assembled hierarchically. These faint stellar halos extend out to the virial radius of the system, and consist mainly of the overlap and mixing of the many “tidal tails” shed by merging progenitors during the assembly of the galaxy. Such origin leads to robust predictions for the dynamics and structure of the outer spheroid that may be contrasted with observation.

- The density profile of the accreted stellar component—which dominates the outer luminous halo—is well approximated by a Sersic-like model where the logarithmic slope steepens monotonically with radius; from $\rho \propto r^{-3}$ near the edge of the galaxy’s traditional luminous boundary to r^{-4} or steeper near the virial radius. The shape and concentration of the accreted component is in reasonable agreement with the Galactic and M31 globular cluster population, lending support to the classic Searle-Zinn scenario for the formation of the globular cluster population.

- The accreted stellar component is reasonably well approximated with a mildly triaxial spheroid with average axis ratios $\langle b/a \rangle \sim 0.91$ and $\langle c/a \rangle \sim 0.84$. Rotation plays a negligible role in the support of the accreted stellar component, which is characterized by a strong radial anisotropy in its velocity distribution. This anisotropy grows from the inside out, from $\sigma_r^2 \sim 2\sigma_t^2$ in the luminous outskirts of the galaxy to $\sigma_r^2 \sim 5\sigma_t^2$ near the virial radius.

- The accreted stellar component is distinct from the dark matter halo as well as from the satellite population, which are typi-

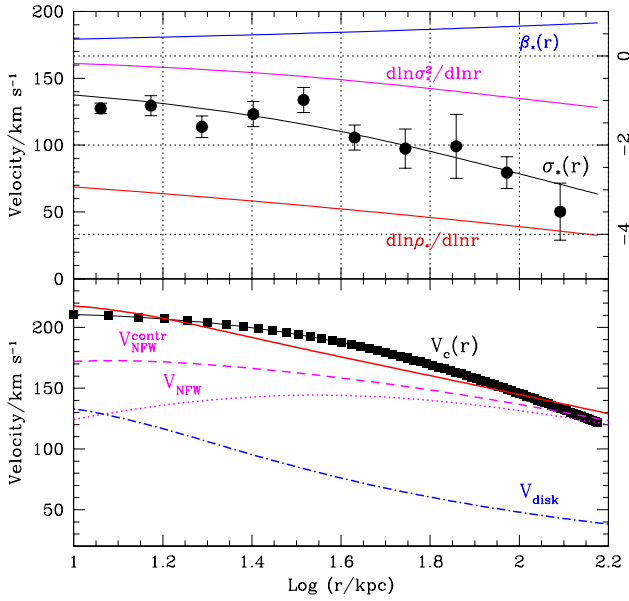


Figure 12. *a-top:* Radial velocity dispersion of Milky Way stellar halo tracers (filled circles, from Battaglia et al 2005). These data are approximated with a simple model where $\sigma_r^2 \propto (1 + r/r_0)^{-2}$, shown by the thin line through the data points. The three other curves (scale at right) illustrate the radial dependence of the right-hand side terms in Jeans' equation (eq. 2), derived assuming a Sersic profile for the tracers. *b-bottom:* Solid squares show the total circular velocity of the Milky Way derived from the top panel. The top solid curve shows a fit assuming an (adiabatically contracted) NFW dark matter halo and an exponential disk. The contribution of the dark matter halo (before and after contraction), as well as that of the disk, are also shown. See text for further details.

cally less concentrated and more isotropic. Most stars in the outer halo formed in progenitors that have since merged with the central galaxy. Only a small fraction of the outer halo stars are contributed through “harassment” of satellites surviving as self-bound entities until the present.

These properties are in broad agreement with recent observations of the outskirts of spiral galaxies as well as of giant stars in the outer regions of the Milky Way and of M31. In particular, they show that the outer light “excess” over extrapolations of the inner luminous profile recently reported for M31 and other spirals is a generic feature of galaxies formed hierarchically, and that the decline in velocity dispersion seen in the outer Milky Way halo tracers is consistent with the presence of an extended, massive halo of dark matter (albeit one of perhaps lower mass than commonly assumed). They also imply that the intergalactic stellar component of galaxy clusters may be more intimately related to the central galaxy than to the galaxy cluster population as a whole. These results illustrate ways to unravel the clues to the tumultuous accretion history of individual galaxies contained in the stars ejected beyond their borders.

ACKNOWLEDGMENTS

We acknowledge useful discussions with Simon White, Stefano Zibetti, and Vincent Eke. We thank Laura Sales for allowing us to quote some of her results in advance of publication and Giuseppe

pina Battaglia for providing the data used in Figure 12 in electronic form. JFN acknowledges support from NSERC, the Canadian Foundation for Innovation, as well as from the Alexander von Humboldt and Leverhulme Foundations.

REFERENCES

- Abadi M. G., Navarro J. F., Steinmetz M., Eke V. R., 2003a, *ApJ*, 591, 499
 Abadi M. G., Navarro J. F., Steinmetz M., Eke V. R., 2003b, *ApJ*, 597, 21
 Bailin, J., & Steinmetz, M. 2004, *ApJ* in press, astro-ph/0408163
 Bailin, J., et al 2005, *ApJL* in press, astro-ph/0505523
 Barnes, J. E., & Hernquist, L. 1992, *ARAA*, 30, 705
 attaglia, G., et al 2005, astro-ph/0506102.
 Brainerd, T. G. 2004, *AIP Conf. Proc.* 743: The New Cosmology: Conference on Strings and Cosmology, 743, 129
 CLewley, L., et al. 2005, *MNRAS*, in press, astro-ph/0506484
 Dekel A., Stoehr F., Mamon G. A., Cox T. J., Primack J. R. 2005, astro-ph/0501622
 Eke, V. R., Navarro, J. F., & Steinmetz, M. 2001, *ApJ*, 554, 114
 Ferguson, A. M. N., Wyse, R. F. G., Gallagher, J. S., & Hunter, D. A. 1998, *ApJL*, 506, L19
 Galletti, S., Federici, L., Bellazzini, M., Fusi Pecci, F., & Macrina, S. 2004, *AA*, 416, 917
 Graham, A. W., & Guzmán, R. 2003, *AJ*, 125, 2936
 Guhathakurta, P. et al 2005, *Nature*, submitted, astro-ph/0502366
 Guzik, J., & Seljak, U. 2002, *MNRAS*, 335, 311
 Hansen, S. & Moore, B., *MNRAS* submitted, astro-ph/0411473.
 Harris, W. E. 1996, *AJ*, 112, 1487
 Helmi, A., & White, S. D. M. 1999, *MNRAS*, 307, 495
 Helmi A., White S. D. M., de Zeeuw P. T., Zhao H., 1999, *Nature*, 402, 53
 Hoekstra, H., Yee, H. K. C., & Gladders, M. D. 2004, *ApJ*, 606, 67
 Ibata R. A., Gilmore G., Irwin M. J., 1994, *Nature*, 370, 194
 Ibata, R., Chapman, S., Ferguson, A. M. N., Irwin, M., Lewis, G., & McConnachie, A. 2004, *MNRAS*, 351, 117
 Irwin, M., et al, 2005, *ApJL*, in press, astro-ph/0505077
 Johnston, K. V., Spergel, D. N., & Hernquist, L. 1995, *ApJ*, 451, 598
 Kazantzidis, S., Kravtsov, A. V., Zentner, A. R., Allgood, B., Nagai, D., & Moore, B. 2004, *ApJL*, 611, L73
 Kennicutt, R. C. 1989, *ApJ*, 344, 685
 Kennicutt R. C., 1998, *ApJ*, 498, 541
 Klypin, A., Zhao, H., & Somerville, R. S. 2002, *ApJ*, 573, 597
 Majewski, S. R., Skrutskie, M. F., Weinberg, M. D., & Ostheimer, J. C. 2003, *ApJ*, 599, 1082
 Martin, C. L., & Kennicutt, R. C. 2001, *ApJ*, 555, 301
 Merritt, D., Navarro, J. F., Ludlow, A., & Jenkins, A. 2005, *ApJL*, 624, L85
 Meza, A., Navarro, J. F., Steinmetz, M., & Eke, V. R. 2003, *ApJ*, 590, 619
 Meza, A., Navarro, J. F., Abadi, M. G., & Steinmetz, M. 2005, *MNRAS*, 359, 93
 Morrison, H. L., Boroson, T. A., & Harding, P. 1994, *AJ*, 108, 1191
 Moore, B., Katz, N., Lake, G., Dressler, A., & Oemler, A. 1996, *Nature*, 379, 613
 Morrison, H. L., Mateo, M., Olszewski, E. W., Harding, P., Dohm-Palmer, R. C., Freeman, K. C., Norris, J. E., & Morita, M. 2000, *AJ*, 119, 2254
 Morrison, H. L., et al. 2003, *AJ*, 125, 2502
 Navarro, J. F., Frenk, C. S., & White, S. D. M. 1996, *ApJ*, 462, 563
 Navarro, J. F., Frenk, C. S., & White, S. D. M. 1997, *ApJ*, 490, 493
 Navarro, J. F., & Steinmetz, M. 1997, *ApJ*, 478, 13
 Navarro, J. F., & Steinmetz, M. 2000, *ApJ*, 528, 607
 Navarro, J. F., et al. 2004, *MNRAS*, 349, 1039
 Romanowsky, A. J., Douglas, N. G., Arnaboldi, M., Kuijken, K., Merrifield, M. R., Napolitano, N. R., Capaccioli, M., & Freeman, K. C. 2003, *Science*, 301, 1696
 Saha, A. 1985, *ApJ*, 289, 310
 Sackett, P. D., Morrison, H. L., Harding, P., & Boroson, T. A. 1994, *Nature*, 370, 441
 Schaye, J. 2004, *ApJ*, 609, 667

- Searle L., Zinn R., 1978, ApJ, 225, 357
Steinmetz, M. 1996, MNRAS, 278, 1005
Steinmetz M., Navarro J. F., 2002, NewA, 7, 155
Zheng, Z., et al. 1999, AJ, 117, 2757
Zibetti, S., White, S. D. M., & Brinkmann, J. 2004, MNRAS, 347, 556
Zibetti, S., White, S. D. M., Schneider, D. P., & Brinkmann, J. 2005, MNRAS, 358, 949
Zinn, R. 1985, ApJ, 293, 424

Table 1. Structural parameters of dark and luminous components of simulated galaxies

Label	r_{vir} kpc	M_{vir} [$10^{11} M_{\odot}$]	M_{drk} [$10^{11} M_{\odot}$]	M_{str} [$10^{11} M_{\odot}$]	M_{glx} [$10^{11} M_{\odot}$]	M_{sat} [$10^{11} M_{\odot}$]	M_{out} [$10^{11} M_{\odot}$]	$f_{\text{glx}}^{\text{acc}}$	$f_{\text{out}}^{\text{acc}}$
KIA1	391.53	29.47	25.96	3.32	2.36	0.47	0.48	0.38	0.91
KIA2	266.41	9.28	7.88	1.29	1.04	0.15	0.10	0.30	0.95
KIA3	267.57	9.41	7.92	1.25	1.02	0.10	0.12	0.42	0.96
KIA4	350.05	21.06	17.96	2.75	1.91	0.51	0.33	0.56	0.94
KIA5	316.30	17.61	15.13	2.25	1.68	0.35	0.23	0.40	0.96
KIB1	394.00	31.53	27.19	3.53	2.60	0.55	0.37	0.39	0.93
KIB2	269.59	9.62	8.18	1.33	1.04	0.17	0.11	0.38	0.97
KIB3	267.83	9.43	7.94	1.23	0.97	0.13	0.12	0.49	0.95

M_{drk} and M_{str} are, respectively, the dark and stellar mass within the virial radius, r_{vir} , defined to encompass a region 100 times denser than the critical density for closure. M_{glx} is the total mass of stars within the luminous radius, $r_{\text{lum}} = 20$ kpc. M_{sat} is the mass of stars in satellites. M_{out} is the mass of stars outside the luminous radius but not in satellites. $f_{\text{glx}}^{\text{acc}}$ and $f_{\text{out}}^{\text{acc}}$ are the fractions of accreted stars in the inner ($r < r_{\text{lum}}$) and outer ($r > r_{\text{lum}}$) galaxy, respectively.

Table 2. Parameters of Sersic-law fits to R -band surface brightness profile of *accreted* stars in the outer ($30 < R/\text{kpc} < 130$) galaxy.

Label	n	R_{eff} kpc	μ_{eff} mag/asec ²	$L_{\text{tot}}^{\text{fit}}$ [$10^{10} L_{\odot}$]	$L_{\text{tot}}^{\text{acc}}$ [$10^{10} L_{\odot}$]
KIA1	5.01	12.41	23.62	3.15	3.68
KIA2	6.13	6.05	23.48	0.85	1.03
KIA3	5.73	5.45	22.93	1.10	1.44
KIA4	5.99	6.33	22.36	2.61	3.52
KIA5	8.27	11.06	24.54	1.23	2.07
KIB1	6.95	8.49	23.10	2.57	3.78
KIB2	6.10	6.07	23.30	1.01	1.32
KIB3	5.96	5.62	23.15	0.97	1.90

$L_{\text{tot}}^{\text{fit}}$ is the total luminosity of the Sersic fit to the outer profile. $L_{\text{tot}}^{\text{acc}}$ is the total luminosity of the accreted stellar component.

